Unlocking the role of pores in chloride permeability of recycled concrete: A multiscale and a statistical investigation

Songsong Lian[a], Shaoqin Ruan[a, b, c]*, Shulin Zhan[a] *, Cise Unluer[d], Tao Meng[a], Kuangliang Qian[a]

[a] College of Civil Engineering and architecture, Zhejiang University, Hangzhou 310058, China

[b] State Key Laboratory of Clean Energy Utilization, Zhejiang University, Hangzhou, 310007, China

[c] State Key Laboratory of Solid Waste Reuse for Building Materials, Beijing, 100041, China

[d] School of Engineering, University of Glasgow, Glasgow, G12 8LT, United Kingdom

Abstract: Chloride ingress is strongly associated with the properties of pores in recycled concrete. To unlock its role in chloride permeability, the pore structures of concrete containing various quantities of recycled coarse (fine) aggregates were analyzed from multi-scales, and the outcomes were further verified by the statistical investigation. The results show that different roles that recycled coarse (fine) played in terms of the pore structures of recycled concrete, as reflected by their volume and diameter of mesopores and micropores, respectively. Meanwhile, Unlike the previous studies, two key pore parameters (i.e., $P_{V<1}$ and P_T) were put forward, revealing their strong interconnections with chloride diffusion of recycled concrete, as confirmed by the statistical analysis. Further, a model concerning chloride permeability of recycled concrete was proposed on a basis of the probability theory, and the newly proposed factor Rp (relied on the previous two pore parameters) has a great relevance to effective chloride diffusion. Therefore, this work enhances accuracy of prediction for chloride diffusivity and durability associated with recycled concrete.

Keywords: Recycled concrete; Pore structure analysis; Chloride penetration; X-ray computed tomography; Correlation analysis

Nomenclature

RCAs: Recycled coarse aggregates

NCAs: Natural coarse aggregates

RFAs: Recycled fine aggregates

NFA: Natural fine aggregate

SP: Superplasticizer

ITZs: Interface transition zones

RCAC: Recycled coarse aggregate concrete

RFAC: Recycled fine aggregate concrete

X-CT: X-ray computed tomography

MIP: Mercury intrusion porosimetry

SEM: Scanning electron microscope

NMR: Nuclear magnetic resonance

D_{Cl^-}: Chloride migration coefficient

1 Introduction

Substitution of natural aggregates with recycled ones to produce concrete enables the production of more sustainable mixtures and facilitates the development of a circular economy [1]. Thus, many countries have encouraged the use of recycled aggregates in a number of applications, and they have been applied in highways, houses and other projects, which attracted widespread attention [2-4]. Recently, scholars have investigated the possibility of using recycled concrete in marine structures [5-6]. However, marine structures are susceptible to the intrusion of chloride, which results in the corrosion of steel bars, the cracking of concrete and ultimately the deterioration of structures [7]. Worse still, the adoption of recycled aggregates for the preparation of concrete was thought to reveal negative impacts on its chloride resistance [8-11], indicating a linear relationship between chloride diffusivity and the replacement ratios of the RCAs [12-14]. Alternatively, Evangelista et al. [15] revealed that when the quantity of the RFAs increased within concrete, an increment rate of 34% was presented in the non-steady-state D_{Cl^-}, as compared with normal concrete. The increased chloride diffusivity of recycled concrete was due to its porous nature associated with the presence of the old mortar attached to the surface of recycled aggregates, bringing about an obvious increase in total porosity that provided the paths for chloride ingress [16-17]. In view of this, chloride ingress is strongly associated with the properties of the pores in recycled concrete, and before any measures that could be taken to enhance the performance of recycled concrete in a marine environment, it is of great significance to reveal the relationship between the pore structure and chloride penetration within recycled concrete.

Certain properties of the pores including size, tortuosity, and total porosity are highly correlated with chloride penetration. Although there have been some attempts to propose relationships between the pore structure and chloride diffusivity within concrete, the outcomes varied among several research groups [18-22]. For example, Zhang et al. [23] demonstrated that there was a close correlation between D_{Cl^-} and pore structure parameters including the total specific pore volume and the most probable pore diameter, as measured by MIP. Besides, the influences of pore size distribution on concrete permeability were reported to be significant [24-25]. Accordingly, pores > 100 nm were thought to increase concrete permeability due to capillary action [26]. The effective chloride diffusivity in mortar can be expressed as a function of capillary porosity and critical porosity, and the model was verified by the experiment results [27]. However, facilitated by MIP and NMR, Zhang et al. [28] also demonstrated that an increase in effective chloride diffusion coefficient was accompanied by the contributive porosity with a pore size between 10–1000 nm and 100–1000 nm, whereas Yang [29] claimed that both the steady-state and non-steady-state D_{Cl^-} were linearly related to the capillary pore volume (i.e. pore diameter of 30-10000 nm) and the critical pore diameter. In addition to the pore size distribution, Wang et al. [30] also put forward an integrated pore index that combined pore tortuosity with pore volume. A prediction model was also established with regard to D_{Cl^-} of recycled concrete, where several complex environmental factors were taken into account.

Research performed in this area so far mainly used MIP and NMR to determine the relationship between the pore structures and chloride diffusivity of concrete, where the properties of the pores were clarified from a microscale. However, existing studies rarely investigated the pore structure of recycled concrete by taking the ITZs into account, which is the region between the aggregate and the paste, and since it will provide more channels for chloride ingress, ITZs is particularly important that determined the performance of recycled concrete. The ITZs in recycled concrete mainly consists of the new ITZs between the old and new mortar, and the old ITZs between the old mortar and aggregates, and the special constitution of RACs may result in different performances of recycled concrete than normal concrete. For instance, chloride diffusivity of recycled concrete increased with the increment of old mortar volume and the old ITZ thickness simultaneously when RCA substitution rates were the same [31-32]. A number of studies investigated the ITZs via the use of nanoindentation [33-35], whereas from a mesoscale, other new approaches such as X-CT are capable of unveiling the correlation between the pore structure and chloride ingress within concrete. Therefore, to provide an improved prediction of chloride diffusivity and durability of recycled concrete, the relationship between the microscopic/mesoscopic structures of recycled concrete and its chloride penetration could be a promising solution.

In this study, the relationship between the pore structure of recycled concrete and chloride penetration was revealed from multi-scales, facilitated by correlation analysis. Finally, information gathered on the pore structures of recycled concrete was used in establishing a mathematical model, where the probability theory was applied.

2 Materials and Methodology

2.1 Materials

The grade of cement used in this study was P·O 42.5, which was manufactured by Anhui Hailuo Cement Co. Ltd, with the chemical compositions shown in **Table 1**. The NFAs (*Apparent density: 2560 kg/m*^{3}*; Fineness modulus: 3.2; Water absorption: 3.5%*) and RFAs (*Apparent density: 2460 kg/m*^{3}*; Fineness modulus: 3.2; water absorption: 10.1%*) were used. The crushed granites with a diameter of 5–25 mm were used as the NCAs (*Apparent density: 2680 kg/m*^{3}*; Water absorption: 0.4%; Crushing index value: 7%*), and the RCAs (*Apparent density: 2580 kg/m*^{3}*; Water absorption: 2.6%; Crushing index value: 11%*) produced by Zhoushan Jinke Resources Recycling Co. Ltd. were used in this study to partially replace the NCAs. The particle size distributions of NCAs, RCAs, NFAs and RFAs were obtained by sieving tests, as presented in **Fig. 1**. As seen from Fig. 1, in order to make the gradation of RCAs approximate to that of NCAs, the obtained RCAs used in this study were carefully selected via the mixing of two kinds of RCAs in a certain proportion.

2.2 Mix proportions and specimen preparation

The w/b ratio was fixed as 0.45; The sand ratio was set as 40%. To prepare RCAC and RFAC, 0, 25 wt.%, 50 wt.%, 75 wt.% and 100 wt.% of NCAs and NFAs were replaced by the RCAs and RFAs. Given the difference in the water absorption between the recycled aggregates and natural aggregates, additional water should be incorporated for the specimen preparation, and the slump was kept between 160 and 200 mm via the use of a superplasticizer. The details of concrete mixtures were presented in **Table 2**. Specimens with the dimensions of Φ100mm*200mm were prepared for a chloride penetration test. For the MIP, X-CT and SEM analysis, the dimensions of 100mm*100mm*100mm were selected. After casting, all the specimens were cured for 24 hours before demoulding, and they were moved to the room with a temperature of 20±2°C and relative humidity of 98±2% for further curing up to 28 days.

2.3 Methodology

2.3.1 Chloride penetration test

According to the Chinese standard GB/T50082-2009 [36], the rapid chloride migration (RCM) test was selected to measure the non-steady state D_{Cl^-} of recycled concrete, as shown in **Fig. 2**. The Φ100mm*200mm specimens were cut into 3 cylindrical specimens with a diameter of (100±1) mm and a height of (50±2) mm. Chloride could penetrate the specimens under an applied constant external voltage (U). After the test, to measure chloride penetration depth (X_d), the specimens were then split along the central axis and sprayed with 0.1 mol of $AgNO_3$ solution. The D_{Cl^-} can be calculated as **Eq. 1**.

$$D_{Cl^-} = \frac{0.0239 \times (273+T)L}{(U-2)t}\left(X_d - 0.0238\sqrt{\frac{(273+T)LX_d}{U-2}}\right) \quad \textbf{Eq. 1}$$

Where U is the absolute value of the voltage (V); T is the average temperature in the solution (°C); L is the thickness of the specimens (mm); t is the test duration (hours).

2.3.2 MIP

The micropores of recycled concrete were determined through a MIP test. The100*100*100 mm specimens were broken into small pieces with a size of 3*3*3 mm, and they were dried at 60°C for 24 hours. The mercury analyzer used for this experiment was an AutoPore IV9510 automatic mercury porosimeter (Micromeritics Instrument Corporation). The pressure from 0.10 to 60000.00 psi was applied for the measurement in this study.

2.3.3 X-CT

The mesopore structures of recycled concrete were determined through an X-CT test. To acquire the X-ray transmission projections, the 100mm*100mm*100mm specimens were scanned by a device, XTH255/320 LC (Nikon, Japan), equipped with a high-resolution detector (2000*2000 pixels). After 3D reconstruction, the image sets were loaded into the software, VGStudio Max 3.0, for pore analysis. To obtained the images, surface determination was carried out after the removal of the background noise. Then, according to the pore analysis module, the properties of each pore inside the specimens including the pore diameter and volume can be acquired.

2.3.4 SEM

Recycled concrete used for SEM were disintegrated into small pieces, and they were dried at 60°C for 24 hours. Those small pieces were sprayed with gold for 60 seconds before SEM analysis. The microstructures of the specimens under different magnifications were observed and captured with an HV-01-43 Field Emission Scanning Electron Microscope (Producer: Sigma, Germany).

2.3.5 Correlation analysis

Correlation analysis is a statistical method to clarify the relationship between different parameters, where the degree of correlation could be revealed. The Pearson's correlation coefficient and Euclidean distance were used as two indicators during the correlation analysis. When studying these two parameters, a greater absolute value of the Pearson correlation coefficient indicates their stronger correlation, whereas a smaller Euclidean distance implies their higher degree of similarity. In this study, the Pearson correlation coefficients and Euclidean distance were calculated by the statistical software, SPSS.

3 Result and Discussion

3.1 Chloride migration coefficient

Fig. 3 shows the D_{Cl^-} of recycled concrete. As expected, the use of the RCAs and RFAs both promoted the chloride diffusion of recycled concrete. Accordingly, as the replacement ratio of the RCAs and RFAs increased, the D_{Cl^-} of recycled concrete significantly increased, which could be related to the inferior properties of old mortar and ITZs [37-38] and the corresponding differences in the pore structures [39]. For instance, when compared with the normal concrete and $C_{100}F_0$, the D_{Cl^-} of RCAC and RCFC increased by 48.2% and 37.4% when the replacement level of the RCAs and RFAs reached 100%, respectively, which were in line with the findings from the previous research [11-15], where an increased rate of the permeability coefficient was seen ranging from 30%-50% and 30%-100% when all the natural aggregates were completely replaced by the natural ones. In view of the previous data and our results, it is difficult to establish a general relationship between the recycled aggregates' quantity and D_{Cl^-}, which could be attributed to the various sources and components of waste concrete used for the manufacturing of the recycled aggregates, and in order to accurately predict the chloride diffusion of recycled concrete, seeking a more universal relationship between its pore structures and D_{Cl^-} could be a possible approach, as elaborated later.

3.2 Pore structure

3.2.1 Micropores

Fig. 4 (a_1), **(b_1)**, **(c_1)** and **(c_2)** show the porosity, average pore diameter and pore size distribution of recycled concrete from a microscale, as acquired from MIP. The figure demonstrates that as the proportion of the RCAs increased, only a slight increase in the total porosity of recycled concrete is observed**,** as revealed in **Fig. 4 (a_2)**, with an average pore diameter of around 18-23 nm. At the same time, the pore size distribution of C_0F_0-$C_{100}F_0$ were also nearly the same **(Fig. 4 (c_3))**, indicating that the different quantities of the RCAs used in recycled concrete preparation failed to alter its pore size distribution. Alternatively, a different trend is seen in the specimens containing various contents of the RFAs with regard to the micropores. For instance, with the growth of the RFAs' content, the porosity of RFAC increased significantly, and the use of the RFAs raised the proportion of the pores with a diameter of ≤100nm, thereby reducing the average pore diameter of RFAC **(Fig. 4 (b_2))**.

Furthermore, according to the classification of the pore diameter, micropores can be divided into 4 groups [40]: (i) Large pores, P_L (>1000 nm); (ii) Capillary pores, P_C (100-1000 nm); (iii) Transitional pores, P_T (10-100 nm); and (iv) Gel pores, P_G (<10 nm). **Fig. 5** shows the volumes of P_L, P_C, P_T and P_G in RCAC and RFAC. For RCAC, the volumes of P_L, P_C, P_T and P_G were very close irrespective of the RCAs' quantity. Alternatively, regarding RFAC, the volumetric increase of P_T and P_G was observed with an increasing RFAs' proportion. Considering the small proportions of P_L and P_C and their negligible variations, the porosity of RFAC containing different quantities of the RFAs mainly depended on the volume of P_T and P_G.

Therefore, from a microscale, the RCAs and RFAs played different roles concerning the pore properties of recycled concrete. To be more specific, the growth in the volume of P_T and P_G increased the porosity and reduced the average pore diameter of RFAC, whereas the structures of the micropores in RCAC remained almost stable regardless of the RCAs' replacement levels.

3.2.2 Mesopores

Through the analysis of the X-CT results, **Fig. 6** shows the distribution and porosity of the mesopores in RCAC and RFAC, where the mesoporosity refers to the volume of mesopores versus the total concrete volume, which is different from the microporosity, where it refers to the volume of micropores versus the total mortar volume. The figure reveals that an increased volume of mesopores in RCAC was accompanied by a rise of the RCAs' quantity, while the mesoporosity of RFAC did not change too much with the variation of the RFAs' content, ranging between 0.66% and 0.70%.

Fig. 7 displays the cumulative number of mesopores in recycled concrete, where rapid growth in the curve is seen initially, followed by a stable trend after the volume of mesopores exceeds 1mm^3. This indicated that in comparison with the mesopores with a volume of ≥ 1mm^3, greater impacts were found in the counterparts with a volume of ≤ 1mm^3 after the addition of recycled aggregates in concrete. Thereby, in order to better analyze the distribution of mesopores with various volumes inside recycled concrete, the pores were marked with different colors according to the pore volume via the X-CT results, as shown in **Fig. 8**. This figure demonstrates that the majority of pores with a volume of ≤ 1mm^3 (marked in blue) were regularly concentrated on the edge of the coarse aggregates, whereas the other pores highlighted in green and red were randomly distributed within the concrete, revealing a volume of ≥ 1mm^3.

Given the volumetric distributions of the pores in the specimens, together with their quantities, the mesopores can be roughly divided into two types, that is, the mesopores with a volume of ≤ 1 mm^3 and ≥ 1mm^3, which were denoted as $P_{V<1}$ and $P_{V>1}$ in this study, respectively (**Fig. 9(a)**). From a mesoscale, when the RCAs' quantity increased, steady growth in the volume of $P_{V<1}$ in RCAC was observed, while its $P_{V>1}$ ranged between 2500 mm^3 to 3000 mm^3, indicating that the volume of $P_{V<1}$ played a pivotal role in the growth of the mesoporosity of RCAC. To be more specific, compared with normal concrete, the $P_{V<1}$ of RCAC increased by more than 50% when the replacement level of the RCAs reached 100%, whereas the $P_{V<1}$ of RFAC remained almost stable irrespective of RFAs ratios (**Fig. 9(b)**). In the case of RFAC, the volume of $P_{V<1}$ was quite stable (i.e. around 3000 mm^3), and as for the volume of $P_{V>1}$, all the values fell in the interval of 2500-3000 mm^3, which seemed insensitive to the quantity of the recycled aggregates, even if all the natural aggregates were replaced by the recycled ones.

The RCAs and RFAs played different roles concerning the pore properties of recycled concrete from multi-scales, which could be related to the difference in the properties of ITZs and old mortar that were attached to the RCAs and RFAs, and more details regarding this aspect will be discussed later.

3.2.3 Morphologies and observations of pores

Although it may not be very accurate, the morphologies of micropores in recycled concrete, including P_T, P_C and P_L could be roughly obtained from **Fig. 10 (a)**, **(b)** and **(c)**, whereas P_G could not be detected through SEM due to its insufficient resolution, as reported earlier [41]. The figure also indicated that the P_T mainly resulted from the gap within the C-S-H particles; the P_C was due to the spacing within the C-S-H agglomerates; the P_L originated from the opening between the C-S-H agglomerates, $Ca(OH)_2$ and Aft. Meanwhile, **Fig. 10 (d)**, **(e)** and **(f)** also show the morphologies of RFAC, demonstrating that the volume of P_T increased when its ratio of the RFAs became increasingly larger. In the meantime, $C_{100}F_0$, $C_{100}F_{50}$ and $C_{100}F_{100}$ revealed a similar distribution of hydration products among them, as reflected by the volume of P_T, indicating that the effects of the RFAs on the morphology and distribution of P_T in recycled concrete could be neglected. Instead, due to the presence of RFAs, the increased P_T were largely associated with the presence of the old mortar on the RFAs, leading to its volumetric growth in recycled concrete.

When it comes to RCAC, the volume of mesopores increased as the content of RCAs surged. In order to better analyze the differences in the mesopores, the cross-sections of natural concrete and recycled concrete were selected, as observed in **Fig. 11 (a)** and **(b)**. The circled areas in the figure indicated the presence of ITZs, where the paste revealed different microstructures from the surrounding mortar due to the high water to cement ratios locally [42]. For both natural concrete and recycled concrete, as expected, a number of mesopores revealing a small volume were concentrated in the ITZs, while many larger mesopores were randomly distributed in the mortar, which was consistent with the X-CT test results. Thus, the substantial $P_{V<1}$ mainly resulted from the ITZs, whether they were from the old mortar attached on the recycled aggregates or from the newly formed concrete **(Fig. 11 (c))**, whereas $P_{V>1}$ could be attributed to the presence of bubbles and some small defects, which is inevitable during concrete preparation.

Consequently, the old ITZs derived from the RCAs brought about an increment of $P_{V<1}$ in recycled concrete than that in natural concrete.

3.3 Correlation analysis

As aforementioned, the chloride diffusivity of recycled concrete was largely relied on its pore structures. Therefore, it is of paramount importance to identify the critical factors that determine chloride permeability in recycled concrete, and the correlation analysis between the D_{Cl^-} and pore structures of recycled concrete became necessary.

According to the outcomes from the MIP, X-CT and SEM analyses, the pores of recycled concrete were classified according to their structures (**Fig. 12**) from multi-scales. For that reason, the correlation analysis between the D_{Cl^-} and pore structure of recycled concrete was performed, where several parameters relating to the micropores and mesopores were taken into account. Concerning the micropores, several parameters including the porosity, average pore diameter, volume of P_L, P_C, P_T and P_G (i.e. V_L, V_C, V_T, and V_G) were considered during the correlation analysis. Alternatively, regarding the mesopores, the relevance of D_{Cl^-} to the porosity, as well as the volume of $P_{V<1}$ and $P_{V>1}$ (i.e. $V_{V<1}$ and $V_{V>1}$) was investigated according to the information obtained in earlier analyses.

Hence, the correlation analysis was conducted based on the relationship between the D_{Cl^-} and each parameter as aforementioned. The results of the Pearson correlation coefficients and Euclidean distance were calculated by the software, SPSS, as listed in **Tables 3** and **4**. As seen from **Table 3**, the D_{Cl^-} of RCAC is greatly associated with the mesoporosity and $V_{V<1}$ at a significance level of 0.01, and the microporosity is also highly related to the D_{Cl^-} at a significant level of 0.05. Therefore, as the correlation coefficient between the D_{Cl^-} of RCAC and $V_{V<1}$ was the largest, whereas their Euclidean distance was minimal, $V_{V<1}$ was identified as the most critical factor that governed the D_{Cl^-} of RCAC.

Regarding RFAC, **Table 4** demonstrates that among all the pore parameters investigated, the D_{Cl^-} is greatly interrelated to the V_T at a significant level of 0.05, with the smallest Euclidean distance revealed by itself as well, defining that the D_{Cl^-} of RFAC is controlled by the V_T.

From a micro- and meso-scale, the decisive factors that governed chloride penetration varied in RCAC and RFAC after the correlation analysis. As for RCAC, derived from the RCAs, the numerous $P_{V<1}$ owing to the presence of old ITZs from the recycled aggregates, as well as the new ITZ between the aggregates and paste, led to an increment of its overall mesoporosity, and as expected, its chloride diffusivity increased linearly with the growth of the $\rho_{V<1}$ (i.e., the porosity of $P_{V<1}$), as shown in **Fig. 13(a)** and **Eq. 2**.

$$D_{Cl^-} = 2.479 + 54.030\rho_{V<1} \qquad \textbf{Eq. 2}$$

As for RFAC, the P_T was identified as the critical factor that determined chloride penetration given the previous analysis, and an increase of the ρ_T (i.e., the porosity of P_T) was accompanied by a linear increase of D_{Cl^-}, as seen in **Fig. 13 (b)** and **Eq. 3.**

$$D_{Cl^-} = 10.306 + 1.273\rho_T \qquad \textbf{Eq. 3}$$

3.4 Discussion

Several studies emphasized that the ITZs and cement paste were influential with the concrete permeability. Therefore, to evaluate the effective diffusivity (i.e., D_{Cl^-} in this study) for concrete, several elementary phases and factors need to be comprehended in advance including chloride diffusivity of the cement paste and ITZs, as well as the volume fraction of aggregates and ITZs [43]. However, as aforementioned, the scenarios of recycled concrete were different compared with the normal cement paste and concrete, as elaborated below.

3.4.1 Relationship between the pore diameter, porosity of cement paste and its D_{Cl^-}

In cement paste, several classic studies [44-45] have revealed a linear relationship between the average pore diameter and the D_{Cl^-}, where the average pore diameter was defined as the pore diameter where half of the pore volume. However, the old mortar attached to the RFAs led to a reduction of the average pore diameter, thus jeopardizing the linear relation between the pore diameter and the D_{Cl^-}.

Meanwhile, as for the relationship between the capillary (gel) porosity and the D_{Cl^-}, Oh and Jang proposed **Eq. 4** and **Eq. 5** as follows [46].

$$\frac{D_{Cl^-}}{D_0} = \rho_{T-por}\frac{\delta}{\tau^2} \quad \textbf{Eq. 4}$$

$$\rho_{T-por} = \rho_{cap} + \rho_{gel} \quad \textbf{Eq. 5}$$

Where $\rho_{T\text{-}por}$ is the total porosity; δ (i..e, tortuosity factor), τ (i.e., constrictivity) and D_0 (i.e., ion diffusivity within water at 25 °C) are constants. ρ_{cap} and ρ_{gel} refer to the porosities of capillary and gel pores, respectively.

ρ_{gel} and ρ_{cap} in **Eq. 5** correspond to ρ_G and the sum of ρ_T and ρ_C in this study, respectively. As seen from the equation, the D_{Cl^-} of recycled concrete was supposed to increase linearly with the growth of $\rho_{T\text{-}por}$. However, in our study, the D_{Cl^-} of RFAC revealed a stronger correlation with the ρ_T than with the $\rho_{T\text{-}por}$ (i.e., ρ_G +ρ_T +ρ_C) and the ρ_{cap} (i.e., ρ_T +ρ_C), as shown in **Fig. 14**, indicating that the crucial factor that governed chloride permeability of RFAC is the P_T instead of other factors, whereas the effects of the P_G and P_C are negligible in terms of the D_{Cl^-} of RFAC. In terms of D_{Cl^-}, the variations between the critical factor that was obtained in this study and from the literature were explained as follows.

There is a consensus as for the influences of the P_G on concrete permeability, as reported in the previous studies [28-30,41], whereas the role of the pores (i.e., a diameter of 100nm-1000nm) played in chloride diffusivity of concrete is much disputed. For instance, Mehta [41] reported that the non-connectivity of small pores could account for a strong correlation between concrete permeability and the pores with a diameter > 100 nm. However, in this study, a different scenario was seen, and due to the old mortar attached to the RFAs, the proportion of the small pores with a diameter of 10~100nm also greatly increased, and the pores with a diameter of 10-100nm that were thought to be isolated in natural concrete could be interconnected in recycled concrete, thereby greatly boost the permeability of RFAC. In view of the foregoing, instead of the capillary, gel or total porosity, the ρ_T through the MIP test could be accurate in the determination of the D_{Cl^-} of RFAC.

3.4.3 Relationship between the porosity of ITZs and its D_{Cl^-}

Unlike cement paste, in natural concrete or mortar, owing to the w/c ratio gradient developed at the interfacial layer, different microstructural images could be observed in the hydrated matrix adjacent to the aggregates [47], that is, ITZs, and Garboczi and Bentz [48] proposed a relationship between the ρ_{ITZs} (i.e., porosity of ITZs) and its D_{Cl^-}, as shown in **Eq. 6**.

$$D_{Cl^-} = D_0(0.001 + 0.07\rho_{ITZs}^2 + 1.8 \cdot H(\rho_{ITZs} - \rho_{cri}) \cdot (\rho_{ITZ} - \rho_{cri})^2) \quad \textbf{Eq. 6}$$

where D_0 a constant as mentioned above; ρ_{ITZs} is the porosity of ITZs; H is the Heaviside function (if x > 0, H(x) = 1, and otherwise, H(x) = 0); ρ_{cri} = 0.18 is the critical porosity at which the pore space disconnected; ρ(x) is the porosity at a distance x from an aggregate surface; dx is the infinitesimal interval of the distance from the aggregate surface; t_{ITZs} is the thickness of the ITZs.

The model proposed by Garboczi and Bentz [48] considered ITZs as a uniform region, which is also proportional to the volume fraction of the aggregate. However, the ITZs are not uniform and its porosity is a variation value along with the distance from the aggregate surface especially in recycled concrete, whose complexity of ITZs is much higher than that of the traditional one, as a result of the old and newly formed ITZs present in recycled concrete. Given this, as the quantity and distribution of ITZs in recycled concrete have great randomness and discreteness, Eq. 6 cannot be directly applied to predict the D_{Cl^-} of the ITZs in recycled concrete, as the relationship between the aggregate volume fraction and ITZ volume fraction is weak.

In consequence, facilitated by X-CT, since $P_{v<1}$ is a sum of pores from the old (from recycled aggregates) and newly formed ITZs, $\rho_{v<1}$ could be a more accurate reflection of its inside D_{Cl^-} rather than ρ_{ITZs} in RCAC, where the D_{Cl^-} can be easily acquired when the $\rho_{v<1}$ is measured.

3.4.4 Relationship between the pore parameters of recycled concrete and its D_{Cl^-}

Given the previous analysis, a strong interconnection between the $\rho_{V<1}/\rho_T$ and the D_{Cl^-} of RCAC/RFAC could be observed, yet in practice, it is inevitable to use both RCAs and RFAs at the same time during the preparation of recycled concrete, and new parameters are required that should consider both the effects of RCAs and RFAs on D_{Cl^-} of recycled concrete.

In view of the foregoing, an increased number of ITZs could be observed with the growth of the RCAs substation level, at the same time, the old mortar attached to the RFAs led to the presence of a large number of P_T, which provided more paths for D_{Cl^-}. Meanwhile, on the premise that the pores are interconnected, a higher concrete porosity could indicate a greater probability of chloride that passes through the pores. Therefore, the probability of chloride that could move through a pore is equivalent to the porosity of a specific type of pore, as shown in **Fig. 15**. Therefore, in this study, the probability of chloride that could pass through the P_T and $P_{V<1}$ of recycled concrete, which were denoted as $PR(P_T)$ and $PR(P_{V<1})$, equaled the ρ_T and $\rho_{V<1}$.

Therefore, from the chances of the potential paths of chloride diffusion within recycled concrete, as shown in **Fig. 15**, a new parameter, R_p, was introduced, which combined the impacts of the $\rho_{V<1}$ and ρ_T on the D_{Cl^-} of recycled concrete simultaneously, and the R_p was obtained through multiplying $\rho_{V<1}$ and ρ_T, as shown in **Eq. 7**, as the chances of two independent events happening together (i.e., chloride that could pass through P_T and $P_{V<1}$ within recycled concrete at the same time) can be calculated by multiplying the chance of each event, as acquired from the classic probability theory.

$$R_p = PR(P_T \cap P_{V<1}) = PR(P_T) \cdot PR(P_{V<1}) = \rho_{V<1} \cdot \rho_T \quad \textbf{Eq. 7}$$

The newly proposed R_p is strongly correlated with chloride diffusion of recycled concrete, as seen from **Fig. 16**. Hence, after measuring the ρ_T and $\rho_{V<1}$ of recycled concrete in practice, its D_{Cl^-} can be well predicted following **Eq. 8**.

$$D_{Cl^-} = 6.344 + 4.452 R_p \quad \textbf{Eq. 8}$$

In a nutshell, compared with the current D_{Cl^-} models, the advantage of the model proposed lied in the consideration of the multiscale pore structures of the cement paste, old and newly formed ITZs in recycled concrete simultaneously, where the critical pore parameters were comprehended separately from a micro- and meso-scale, thus the prediction accuracy of the D_{Cl^-} model for the recycled concrete is greatly enhanced.

4. Conclusion

Compared with the natural aggregates, the use of recycled ones revealed different impacts on D_{Cl^-}, which is owing to their multiscale pore structures caused by the addition of the RCAs/RFAs, highlighting their importance with respect to the prediction of the D_{Cl^-} and durability of recycled concrete. Further, RCAs/RFAs played different roles with regard to the pore structures of recycled concrete in a micro- and meso-scale, which can be assigned to the old ITZs attached on the RCAs that led to an increase of $P_{V<1}$ from a meso-scale, as well as the volumetric growth of P_T and P_G due to the addition of RFAs from a micro-scale.

Finally, in view of the multi-structures of the cement paste, old and newly formed ITZs, the new parameter derived from the probability theory revealed great accuracy in predicting the D_{Cl^-} and durability of recycled concrete, where the $\rho_{V<1}$ and ρ_T were identified to be strongly related to its D_{Cl^-} based on different scales, and the higher accuracy of the D_{Cl^-} prediction may promote the usage of recycled concrete in practice, especially in a chloride-rich environment.

Acknowledgement

The authors gratefully acknowledge the support from Zhejiang Provincial Key Laboratory of Marine Geotechnical Engineering and Materials. Financial support from State Key Laboratory of Solid Waste Reuse for Building Materials (SWR-2021-004) and State Key Laboratory of Clean Energy Utilization, Zhejiang University (109203*A62103/027) is also acknowledged.

List of Tables

Table 1 Chemical composition of cement

Composition	Al_2O_3	SiO_2	CaO	Fe_2O_3	SO_3	MgO	f-CaO
Wt. (%)	4.36	22.37	61.08	3.38	2.45	2.43	0.86

Table 2 Mix proportions of concrete (kg/m^3)

	Cement	Water	NCAs	RCAs	NFAs	RFAs	Additional water	SP
C_0F_0	400	180	1095	0	730	0	0	1.6
$C_{25}F_0$	400	180	821	274	730	0	6	1.6
$C_{50}F_0$	400	180	547.5	547.5	730	0	12	1.6
$C_{75}F_0$	400	180	274	821	730	0	18	1.6
$C_{100}F_0$	400	180	0	1095	730	0	24	1.6
$C_{100}F_{25}$	400	180	0	1095	547.5	182.5	36	1.6
$C_{100}F_{50}$	400	180	0	1095	365	365	48	1.6
$C_{100}F_{75}$	400	180	0	1095	182.5	547.5	60	1.6
$C_{100}F_{100}$	400	180	0	1095	0	730	72	1.6

C_x: The replacement level of natural coarse aggregates by the recycled ones；

F_x: The replacement level of natural fine aggregates by the recycled ones；

Table 3 Correlation analysis between the D_{Cl^-} and pore parameters of RCAC

Parameters	Micropores						Mesopores		
	Porosity	Average Pore Diameter	V_G	V_T	V_C	V_L	Porosity	$V_{v<1}$	$V_{v>1}$
Correlation coefficient	0.887*	0.280	0.105	0.106	0.564	0.658	0.985**	0.996**	0.467
Euclidean distance	0.952	2.401	2.675	2.674	1.867	1.654	0.345	0.171	2.066

** Represents that the correlation is remarkable at a significance level of 0.01.

*Represents that the correlation is remarkable at a significance level of 0.05.

Table 4 Correlation analysis between the D_{Cl^-} and pore parameters of RFAC

Parameters	Micropores						Mesopores		
	Porosity	Average Pore Diameter	V_G	V_T	V_C	V_L	Porosity	$V_{v<1}$	$V_{v>1}$
Correlation coefficient	0.837	-0.279	0.530	0.943*	-0.557	-0.766	-0.171	-0.493	0.081
Euclidean distance	1.142	3.199	1.940	0.673	3.529	3.759	3.061	3.456	2.711

** Represents that the correlation is remarkable at a significance level of 0.01.

* Represents that the correlation is remarkable at a significance level of 0.05.

List of Figures

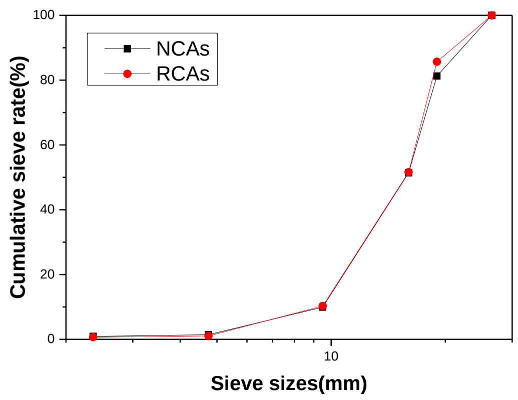

(a)

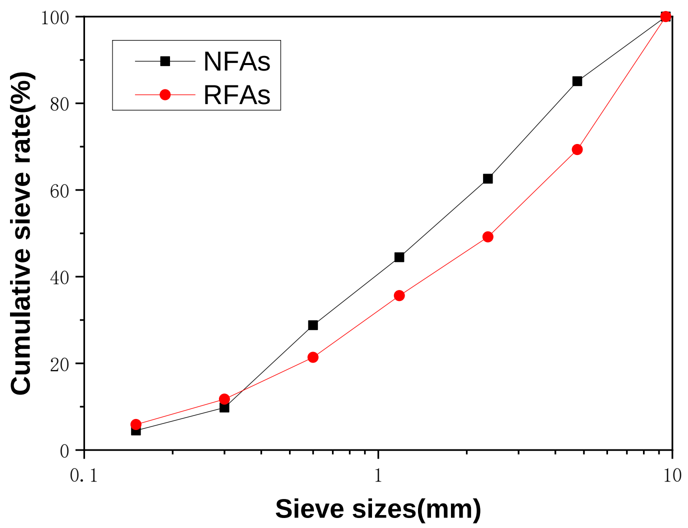

(b)

Fig. 1 Particle size distributions of aggregates: (a) Coarse aggregate; (b) Fine aggregate

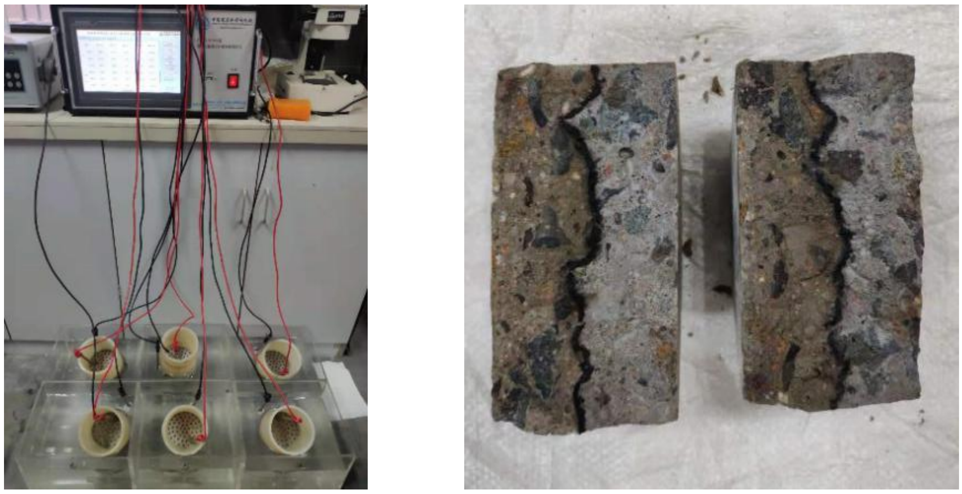

(a) (b)

Fig. 2 Rapid chloride migration test: (a) Test equipment; and (b) specimens sprayed with $AgNO_3$ solution

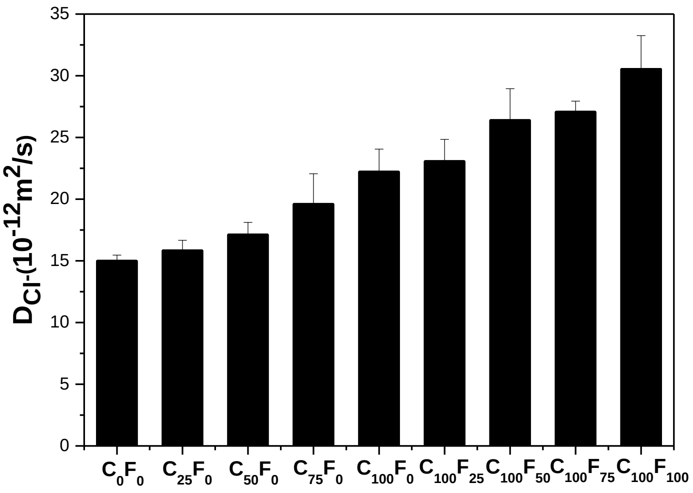

(a)

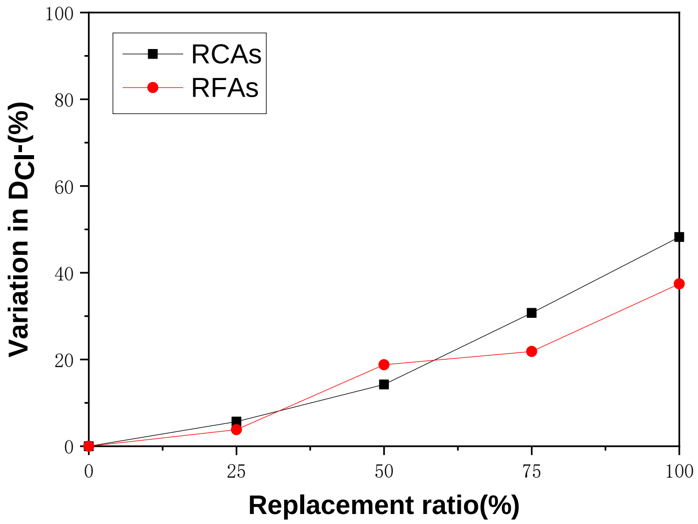

(b)

Fig. 3 (a) D_{Cl^-} and (b) variation in D_{Cl^-} of recycled concrete

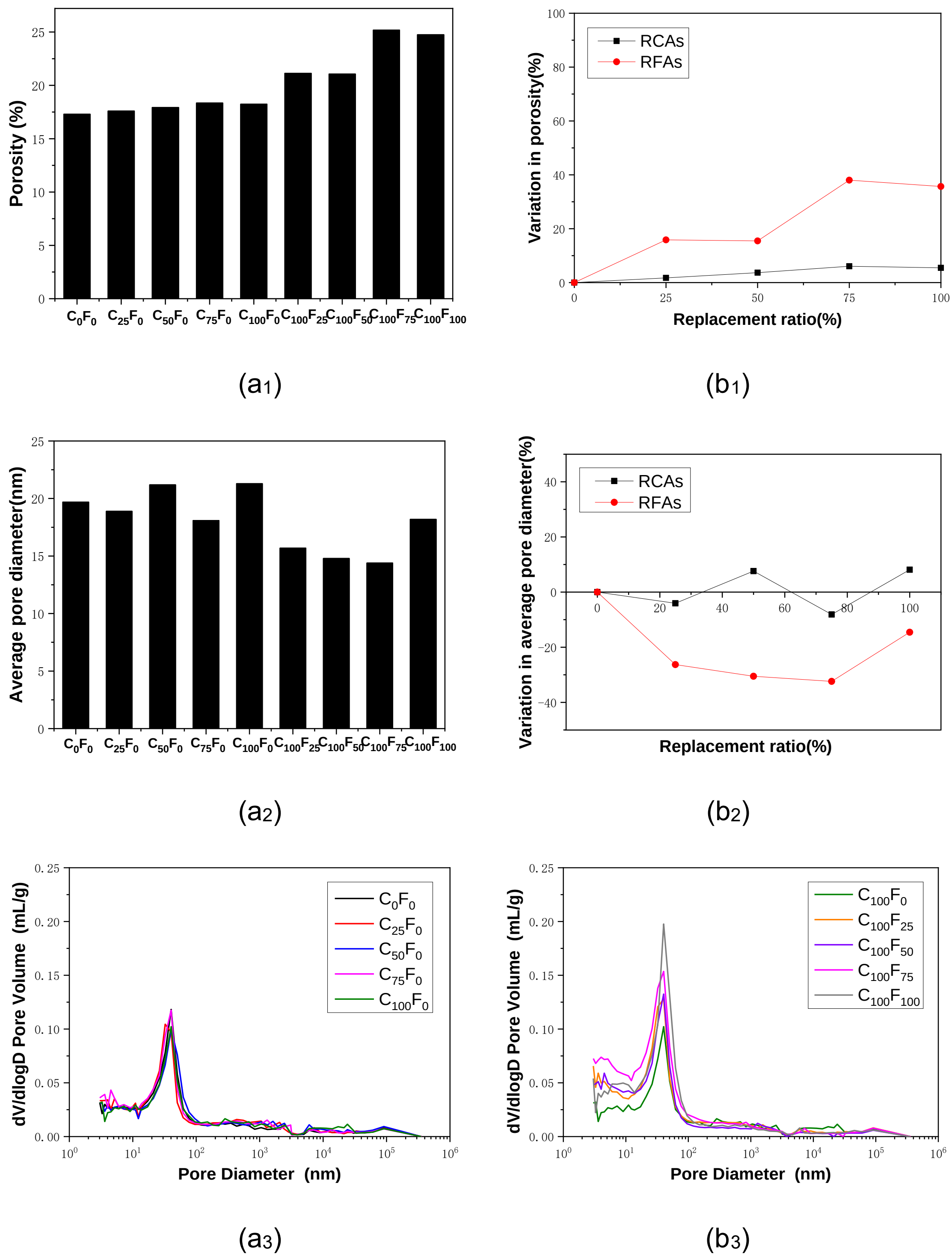

Fig. 4 (a_1)~(b_1) Porosity and its variation, (a_2)~ (b_2) average pore diameter and its variation in recycled concrete, as well as pore size distribution of (a_3) RCAC and (b_3) RFAC

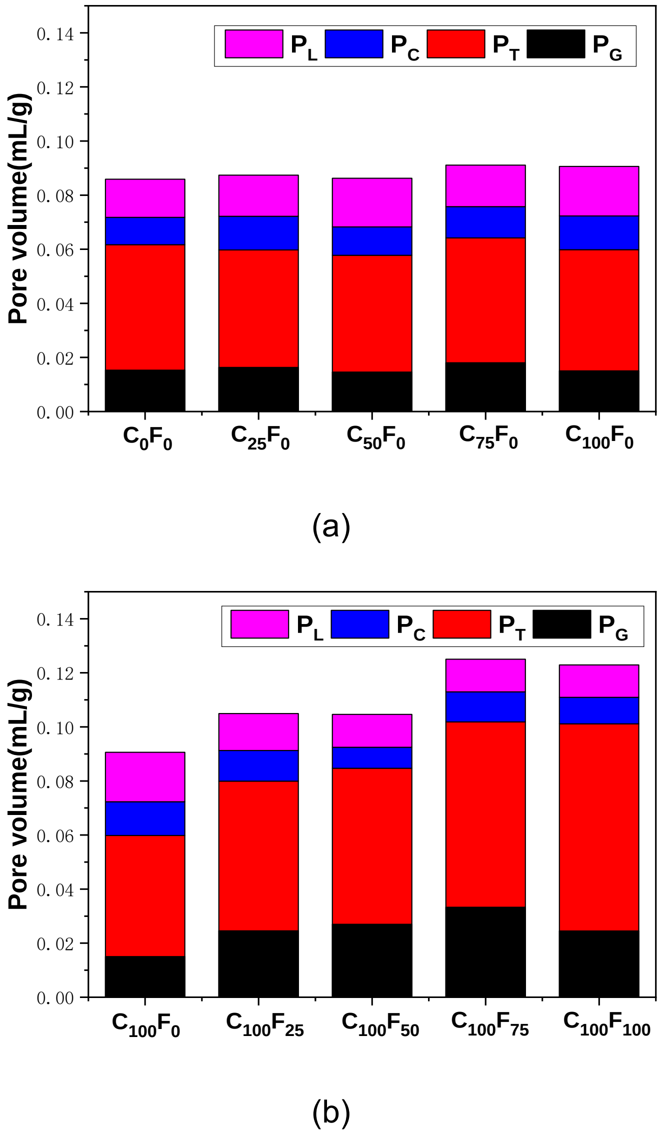

Fig. 5 Volumes of P_L, P_C, P_T and P_G in (a) RCAC and (b) RFAC

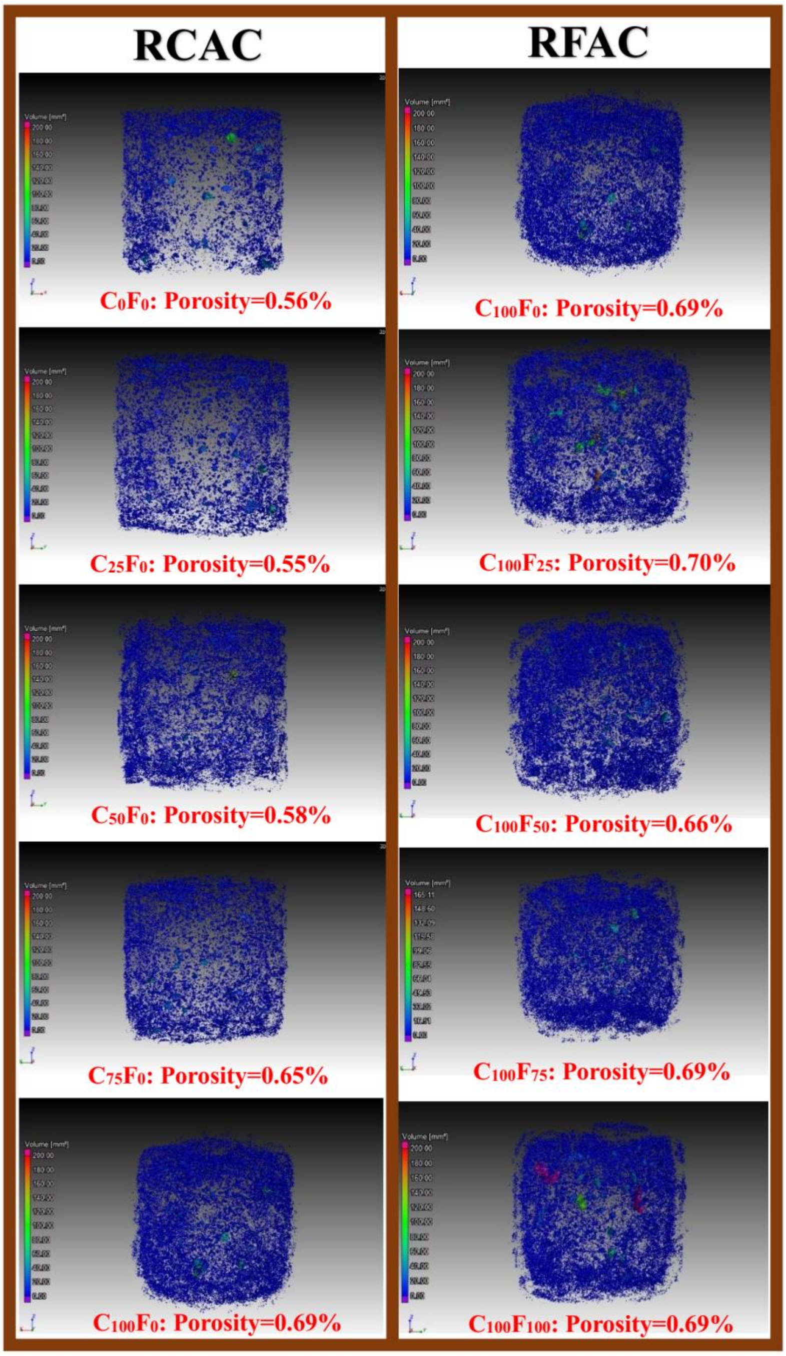

Fig. 6 3D diagram of mesopore distribution in RCAC and RFAC

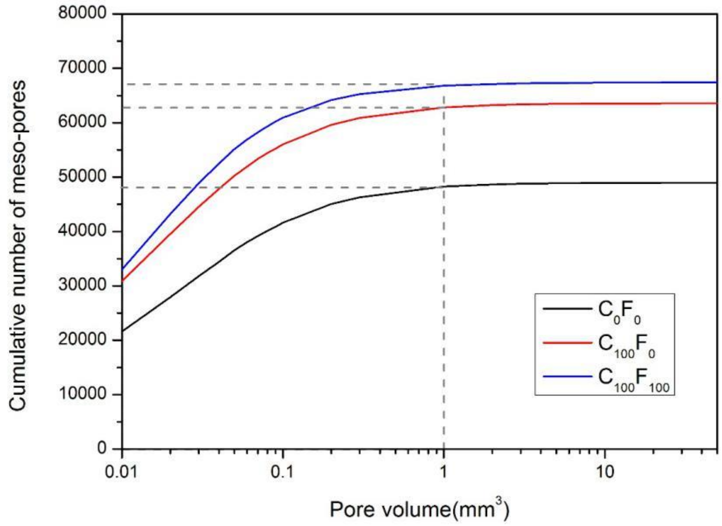

Fig. 7 Cumulative number of mesopores

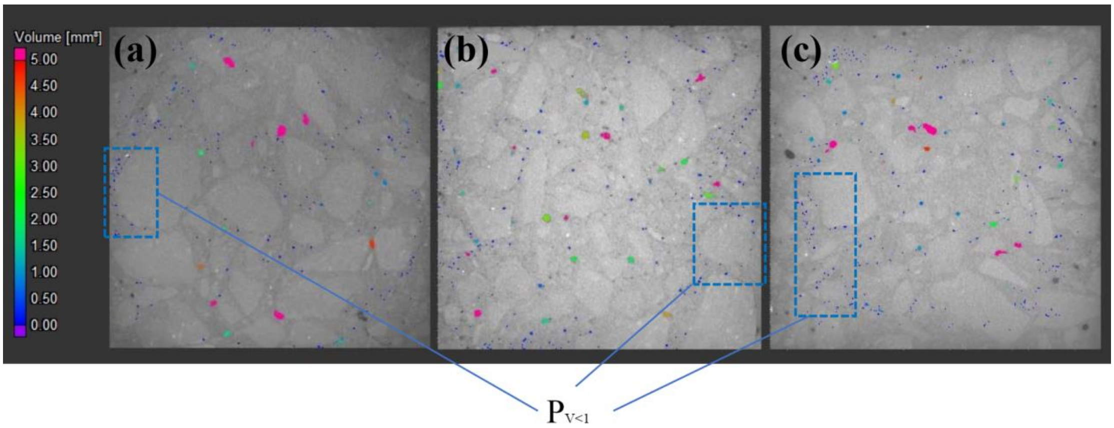

Fig. 8 Pores with different volumes on the cross-sections of (a) C_0F_0, (b) $C_{100}F_0$ and (C) $C_{100}F_{100}$

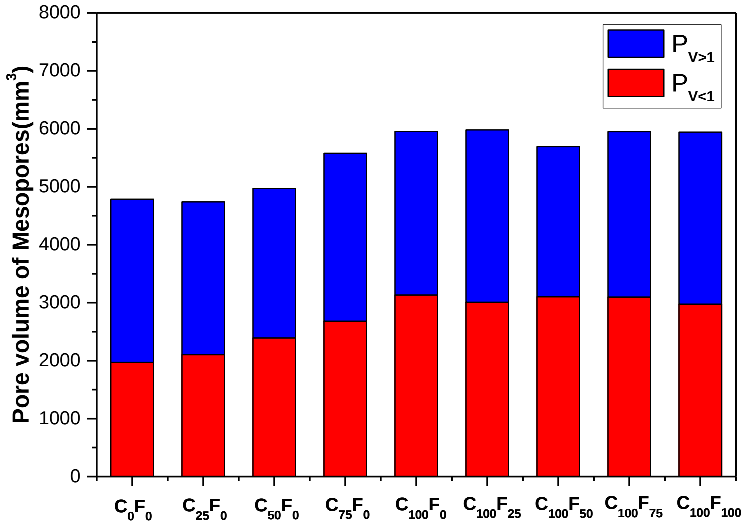

(a)

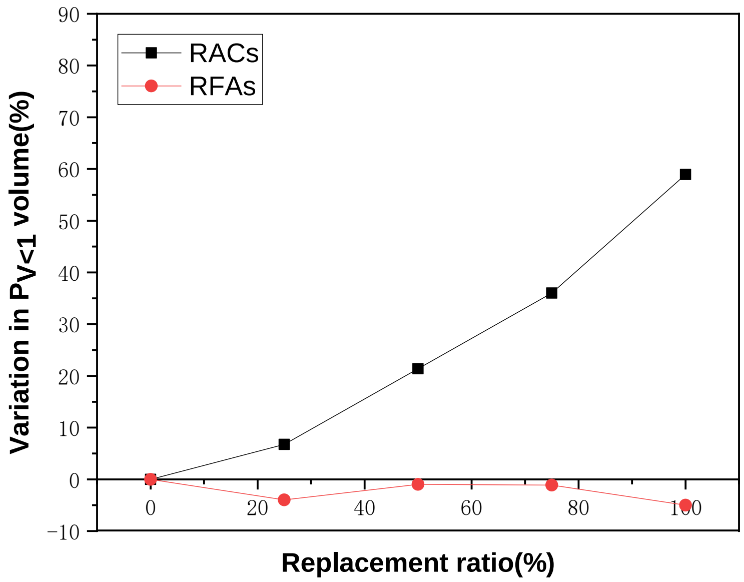

(b)

Fig. 9 Mesopores within recycled concrete: (a)$P_{V<1}$ and $P_{V>1}$; and (b) variation in $P_{V<1}$ volume

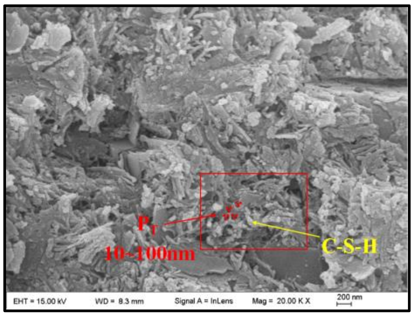

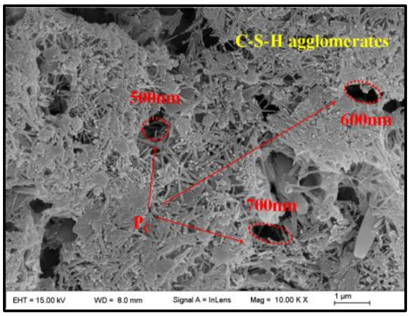

(a) (b)

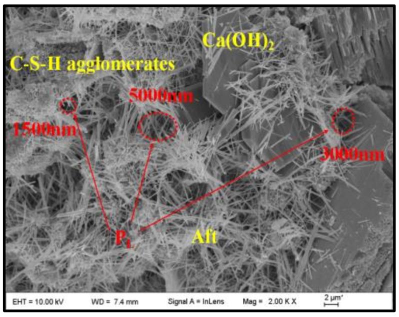

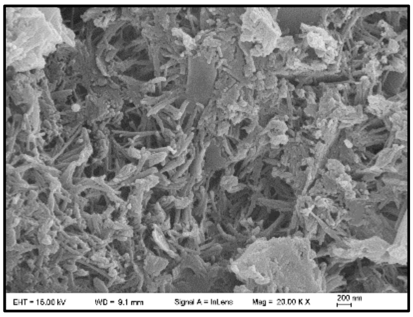

(c) (d)

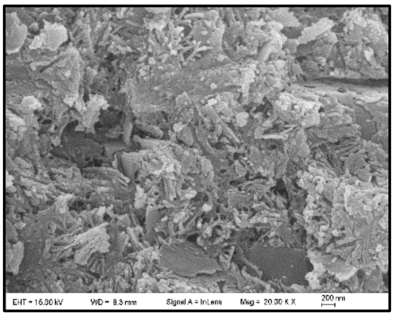

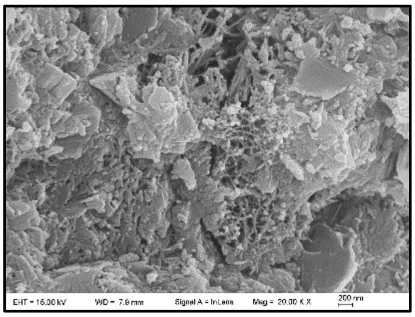

(e) (f)

Fig. 10 Morphologies of micropores (Magnification: 2k): **(a)** P_T, **(b)** P_C and **(c)** P_L; Morphologies of RFAC: **(d)** $C_{100}F_0$, **(e)** $C_{100}F_{50}$, and **(f)** $C_{100}F_{100}$ (Magnification: 20k)

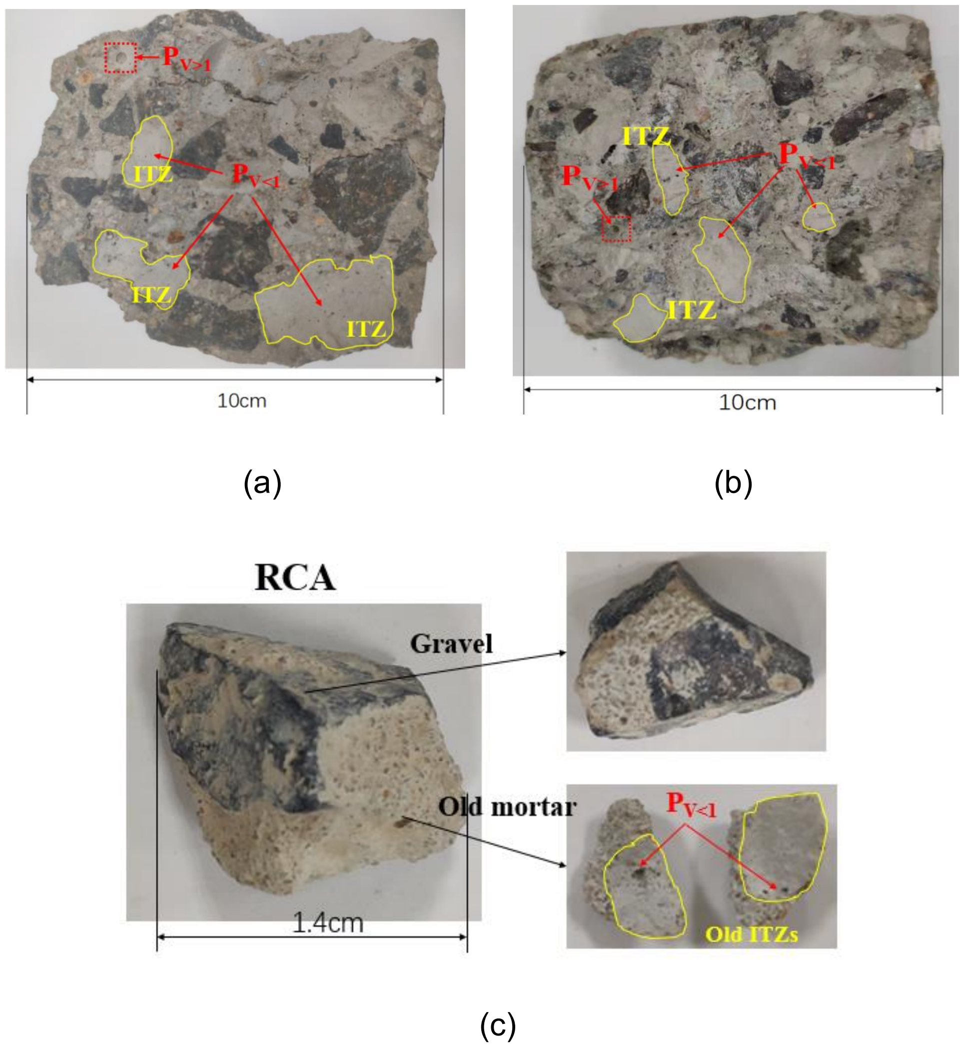

Fig. 11 Observations of cross-sections **(a)** C_0F_0, **(b)** $C_{100}F_0$ and **(c)** RCAs

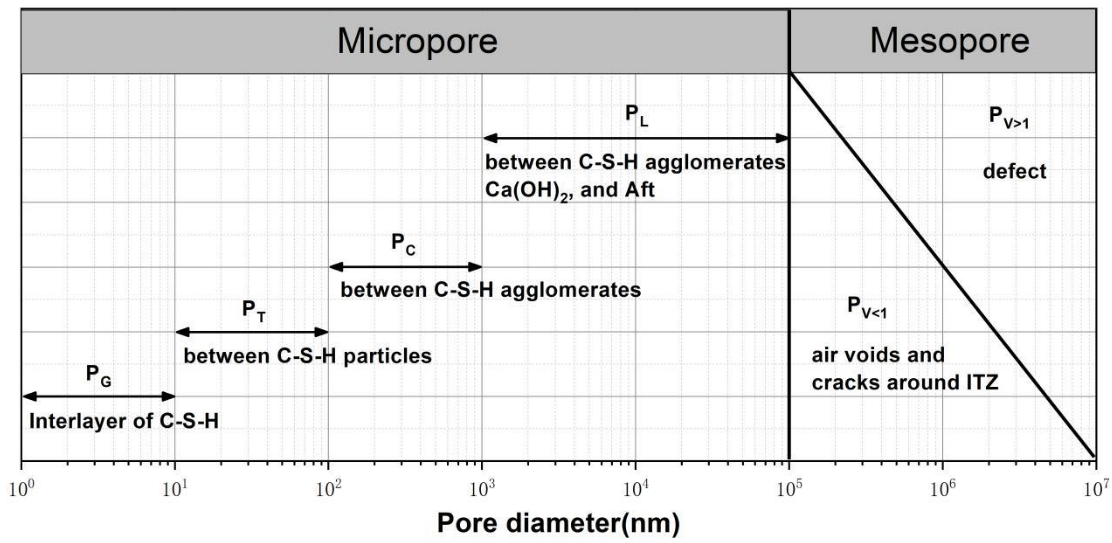

Fig. 12 Classification of pores in recycled concrete

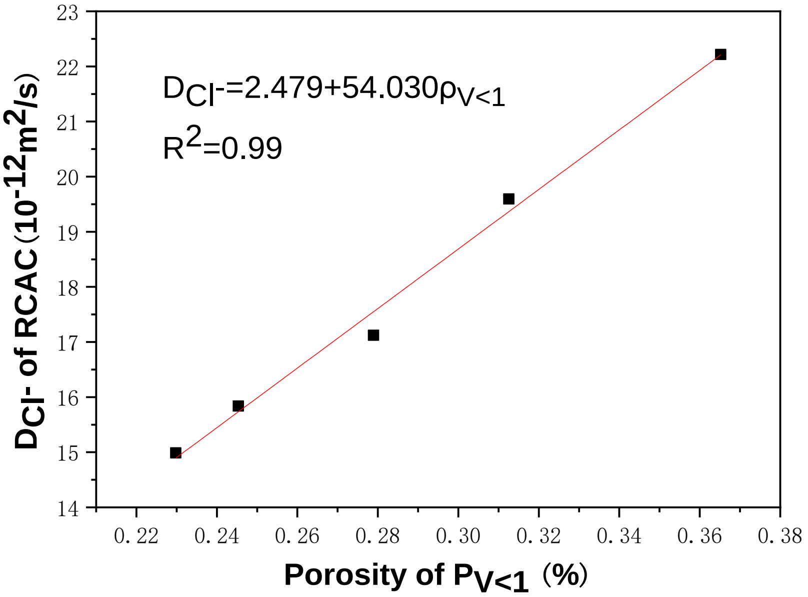

(a)

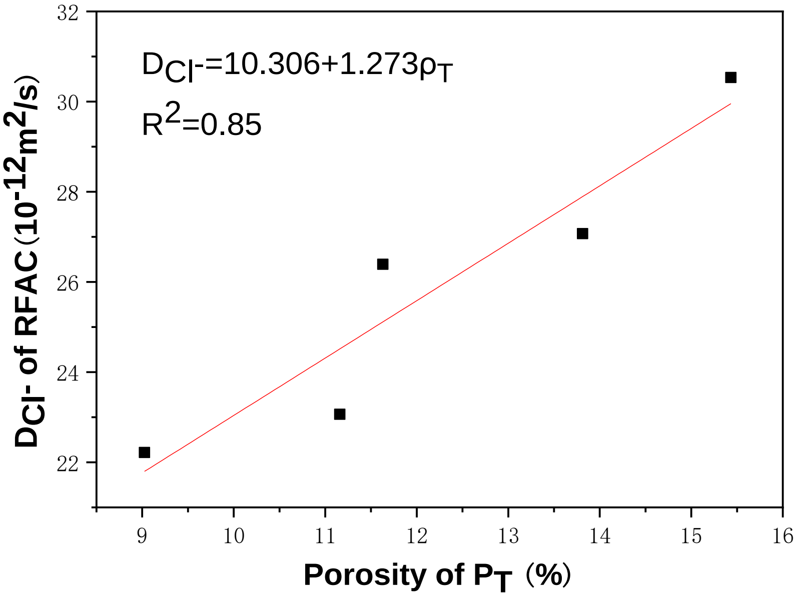

(b)

Fig. 13 Relationship between **(a)** the D_{Cl^-} of RCAC and the $\rho_{V<1}$; **(b)** the D_{Cl^-} of RFAC and the ρ_T

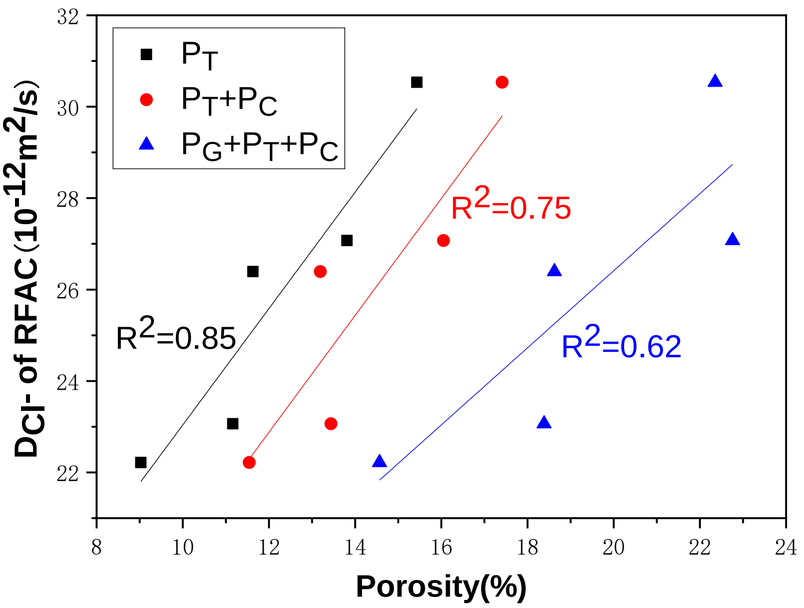

Fig. 14 Relationship between the porosity of different types of pores and the D_{Cl^-}

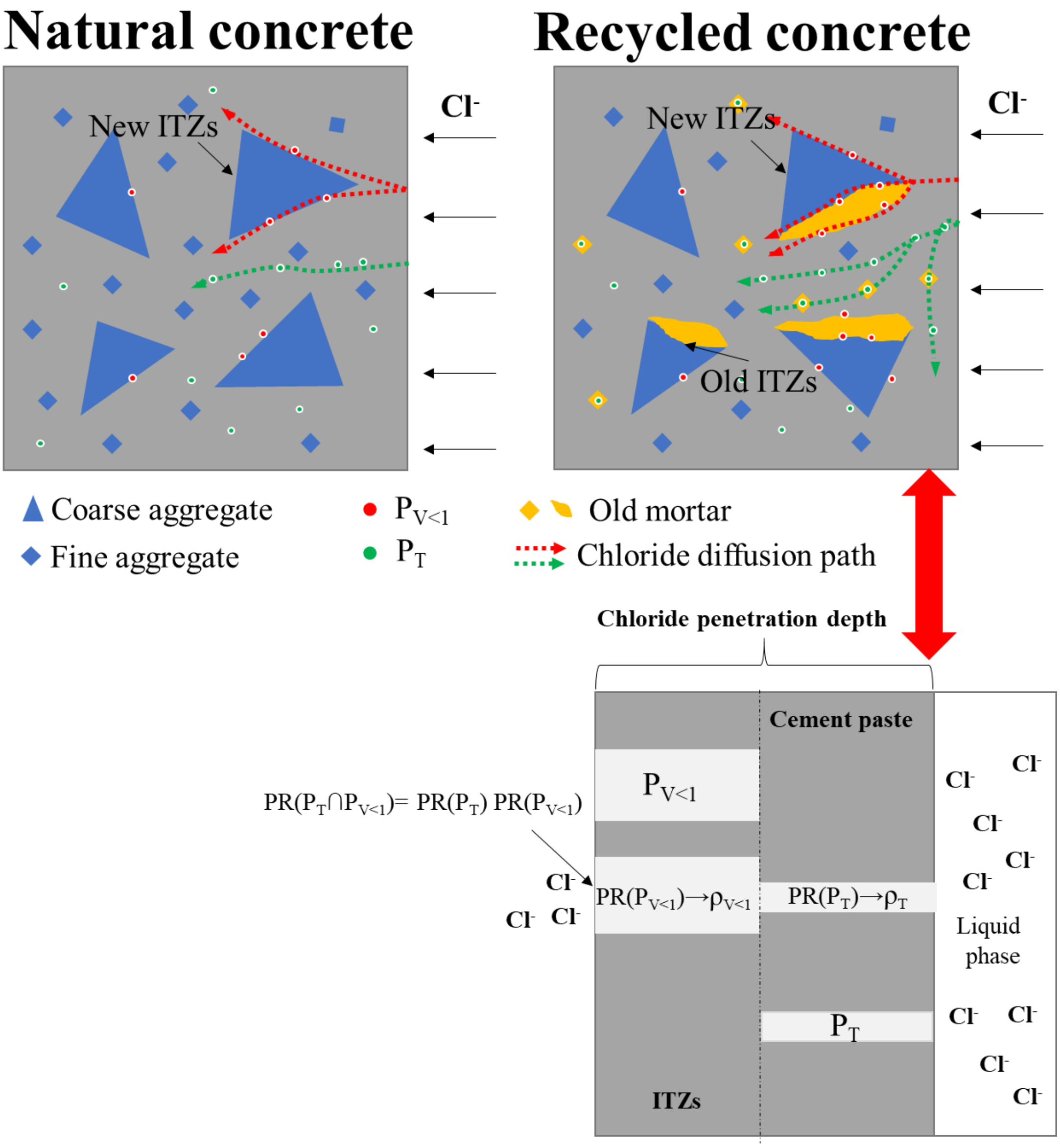

Fig. 15 Illustration of the probability of chloride diffusivity into natural and recycled concrete given its possible diffusion channels

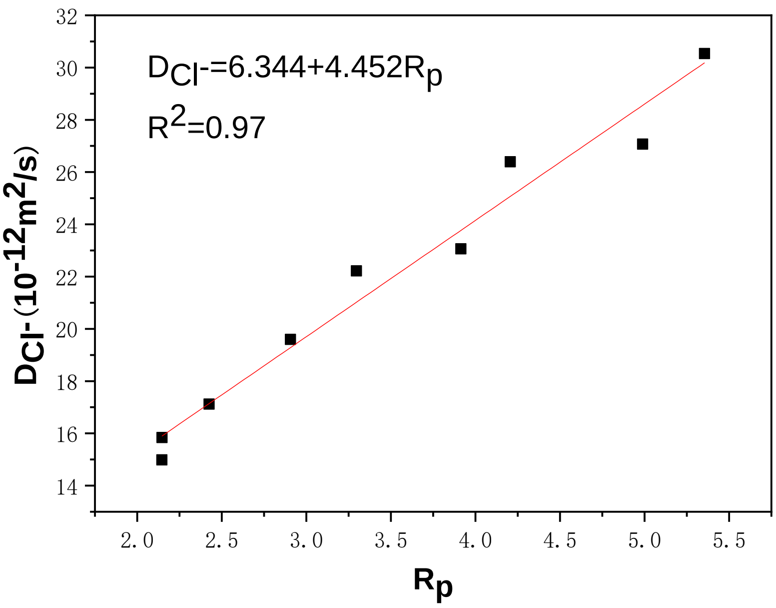

Fig. 16 Relationship between the R_p and the D_{Cl^-} of all the specimens

References

[1] L.A. Lopez Ruiz, X. Roca Ramon and S. Gasso Domingo, The circular economy in the construction and demolition waste sector - A review and an integrative model approach, J. Clean. Prod. 248(2020) 119238.

[2] C. Poon and D. Chan, The use of recycled aggregate in concrete in Hong Kong, Resour. Conserv. Recy. 50(2007) 293-305.

[3] Q. Tang, Z.M. Ma, H.X. Wu, W. Wang, The utilization of eco-friendly recycled powder from concrete and brick waste in new concrete: A critical review, Cem. Concr. Compos. 114(2020) 103807.

[4] C. Thomas, J. Setien, J.A. Polanco, A.I. Cimentada and C. Medina, Influence of curing conditions on recycled aggregate concrete, Constr. Build. Mater. 172(2018) 618-625.

[5] S. Ismail, M. Ramli. Mechanical Properties of Concrete Using Treated Recycled Concrete Aggregate in Marine Environment. Key. Eng. Mater. 841(2020) 138-143.

[6] W. Chalee, T. Cheewaket, C. Jaturapitakkul, Utilization of Recycled Aggregate Concrete for Marine Site Based on 7-Year Field Monitoring, Int. J. Concr. Struct. Mater. 15(2021) 34.

[7] W. V. Srubar, Stochastic service-life modeling of chloride-induced corrosion in recycled-aggregate concrete. Cem. Concr. Compos. 55(2015) 103-111.

[8] D. Pedro, J. de Brito, L. Evangelista, Durability performance of high-performance concrete made with recycled aggregates, fly ash and densified silica fume, Cem. Concr. Compos. 93(2018) 63-74.

[9] J. Bao, S. Li, P. Zhang, X. Ding, S. Xue, Y. Cui and T. Zhao, Influence of the incorporation of recycled coarse aggregate on water absorption and chloride

penetration into concrete, Constr. Build. Mater. 239(2020) 117845.

[10] J. Xiao, D. Lu, J. Ying, Durability of recycled aggregate concrete: an overview. J. Adv. Concr. Technol. 11(12) (2013) 347-359.

[11] H. Guo, C. Shi, X. Guan, J. Zhu, Y. Ding, T. C. Ling, et al. Durability of recycled aggregate concrete–a review. Cem. Concr. Compos. 89(2018) 251-259.

[12] W. Dodds, C. Goodier, C. Christodoulou, S. Austin, D. Dunne, Durability performance of sustainable structural concrete: Effect of coarse crushed concrete aggregate on microstructure and water ingress, Constr. Build. Mater. 145 (2017) 183–195.

[13] A.J. Chen, J. Wang, Z.F. Ge, M. Wu, The Durability Life Prediction of Recycled Concrete under Chlorate Environment, Adv. Mater. Res. 314 (2011) 849–852.

[14] N.S. Amorim Junior, G.A.O. Silva, C.M.R. Dias and D.V. Ribeiro, Concrete containing recycled aggregates: Estimated lifetime using chloride migration test, Constr. Build. Mater. 222(2019) 108-118.

[15] L. Evangelista and J. de Brito, Durability performance of concrete made with fine recycled concrete aggregates, Cem. Concr. Compos. 32(2010) 9-14.

[16] H. Qin, Y. Yang, Influence of the interfacial transition zone on anti chloride ion permeability of recycled concrete, Highway. Eng. 41 (2016) 70–74.

[17] J.X. Lu, P.L. Shen, H.B. Zheng, B.J. Zhan, H.A. Ali, P.P. He, C.S. Poon, Synergetic recycling of waste glass and recycled aggregates in cement mortars: Physical, durability and microstructure performance, Cem. Concr. Compos. 113(2020) 103632.

[18] M.S. Sumanasooriya, N. Neithalath, Pore structure features of pervious

concretes proportioned for desired porosities and their performance prediction, Cem. Concr. Compos. 33 (8) (2011),778-787.

[19] G. Ye, Percolation of capillary pores in hardening cement pastes, Cem. Concr. Res. 35 (1) (2005), 167-176.

[20]Y. Zhou, D. Hou, J. Jiang, P. Wang, Chloride ions transport and adsorption in the nano-pores of silicate calcium hydrate: Experimental and molecular dynamics studies, Constr. Build. Mater. 126 (2016) 991-1001.

[21]M.K. Mohammed, A.R. Dawson, N.H. Thom, Macro/micropore structure characteristics and the chloride penetration of self-compacting concrete incorporating different types of filler and mineral admixture, Constr. Build. Mater. 72 (72) (2014), 83-93.

[22] J. Ying, Z. Han, L. Shen, W. Li, Influence of parent concrete properties on compressive strength and chloride diffusion coefficient of concrete with strengthened recycled aggregates, Mater. 13(20) (2020), 4631.

[23] M. Zhang and H. Li, Pore structure and chloride permeability of concrete containing nano-particles for pavement, Constr. Build. Mater. 25(2011) 608-616.

[24] B.B. Das and B. Kondraivendhan, Implication of pore size distribution parameters on compressive strength, permeability and hydraulic diffusivity of concrete, Constr. Build. Mater. 28(2012) 382-386.

[25] N. Neithalath, M.S. Sumanasooriya and O. Deo, Characterizing pore volume, sizes, and connectivity in pervious concretes for permeability prediction, Mater. Charact. 61(2010) 802-813.

[26] M. Oltulu and R. Sahin, Pore structure analysis of hardened cement mortars containing silica fume and different nano-powders, Constr. Build. Mater. 53(2014) 658-664.

[27] J. Ying, B. Zhou, J. Xiao, Pore structure and chloride diffusivity of recycled aggregate concrete with nano-SiO_2 and nano-TiO_2, Constr. Build. Mater. 150 (2017) 49–55.

[28] J. Zhang, F. Bian, Y. Zhang, Z. Fang, C. Fu and J. Guo, Effect of pore structures on gas permeability and chloride diffusivity of concrete, Constr. Build. Mater. 163(2018) 402-413.

[29] C.C. Yang, On the relationship between pore structure and chloride diffusivity from accelerated chloride migration test in cement-based materials, Cem. Concr. Res. 36(2006) 1304-1311.

[30] J. Wang, J. Zhang and D. Cao, Pore characteristics of recycled aggregate concrete and its relationship with durability under complex environmental factors, Constr. Build. Mater. 272(2021) 121642.

[31] Y. Wu, J. Xiao, Multiscale digital-image driven stochastic finite element modeling of chloride diffusion in recycled aggregate concrete, Constr. Build. Mater. 162 (2018) 239–252.

[32] J. Ying, J. Xiao, V.W.Y. Tam, On the variability of chloride diffusion in modelled recycled aggregate concrete, Constr. Build. Mater. 41(2013) 732–741.

[33] Y. Zhou, W. She, D. Hou, B. Yin, H. Chang, J. Jiang, et al. Modification of incorporation and in-situ polymerization of aniline on the nano-structure and meso-structure of calcium silicate hydrates, Constr. Build. Mater. 182(2018) 459-468.

[34] C. R. Wu, Z. Q. Hong, J. L. Zhang, S. C. Kou, Pore size distribution and ITZ performance of mortars prepared with different bio-deposition approaches for the treatment of recycled concrete aggregate, Cem. Concr. Compos. 111(2020) 103631.

[35] P. J. M. Monteiro, G. Geng, D. Marchon, J. Li, M.J.A. Qomi, Advances in characterizing and understanding the microstructure of cementitious materials, Cem. Concr. Res. 124(2019)105806.

[36] China National Standards. Standard for test methods of long-term performance and durability of ordinary concrete. GB/T50082-2009.

[37] N. Otsuki, S. Miyazato, W. Yodsudjai, Influence of recycled aggregate on interfacial transition zone, strength, chloride penetration and carbonation of concrete, J. Mater. Civ. Eng. 15 (5) (2003) 443–451.

[38] R. Muduli, B.B. Mukharjee, Performance assessment of concrete incorporating recycled coarse aggregates and metakaolin: A systematic approach, Constr. Build. Mater. 233 (2020) 117223.

[39] C. Liang, Z. Cai, H. Wu, J. Xiao, Y. Zhang, Z. Ma, Chloride transport and induced steel corrosion in recycled aggregate concrete: A review, Constr. Build. Mater. 282(2021) 122547.

[40] S. Jin, J. Zhang, S. Han, Fractal analysis of relation between strength and pore structure of hardened mortar. Constr. Build. Mater. 135(2017) 1-7.

[41] P. K. Mehta. Concrete: Microstructure, Properties and Materials. 3rd ed. New York: MeGraw Hill, 2005.

[42] J. P. Ollivier, J. C. Maso, B. Bourdette, Interfacial transition zone in concrete. Adv. Cem. Based. Mater. 2(1) (1995) 30-38.

[43] G. Sun, Y. Zhang, S. Wei, Z. Liu, C. Wang, Multi-scale prediction of the effective chloride diffusion coefficient of concrete, Constr. Build. Mater. 25(10) (2011) 3820-3831.

[44] P. Halamickova, R. J. Detwiler, D. P. Bentz, E. J. Garboczi, Water permeability and chloride ion diffusion in Portland cement mortars: relationship

to sand content and critical pore diameter, Cem. Concr. Res. 25.4 (1995) 790-802.

[45] D.M. Roy, Relationship Between Permeability, Porosity, Diffusion and Microstructure of Cement Pastes, Mortar, and Concrete at Different Temperatures, Materials Research Society Symposium Proceedings, 137(1988) 179.

[46] Oh, Byung Hwan, Seung Yup Jang. Prediction of diffusivity of concrete based on simple analytic equations. Cem. Concr. Res. 34(3) (2004) 463-480.

[47] C.C. Yang, J.K. Su, Approximate migration coefficient of interfacial transition zone and the effect of aggregate content on the migration coefficient of mortar, Cem. Concr. Res. 32(10) (2002):1559–65.

[48] E. J. Garboczi, D. P. Bentz, Multi-scale analytical/numerical theory of the diffusivity of concrete. Adv. Cem. Based. Mater. 8(2) (1998) 77-88.